Available online at www.sciencedirect.com

SCIENCE DIRECT®

Journal of Molecular Catalysis A: Chemical 203 (2003) 267–275

JOURNAL OF MOLECULAR CATALYSIS A: CHEMICAL

www.elsevier.com/locate/molcata

Liquid phase hydrogenation of furfural to furfuryl alcohol over the Fe-promoted Ni-B amorphous alloy catalysts

Hexing Li [a,*], Hongshan Luo [a], Li Zhuang [a], Weilin Dai [b], Minghua Qiao [b]

[a] *Department of Chemistry, Shanghai Normal University, Shanghai 200234, PR China*
[b] *Department of Chemistry, Fudan University, Shanghai 200433, PR China*

Received 13 January 2003; received in revised form 10 April 2003; accepted 10 April 2003

Abstract

The ultrafine Fe-doped Ni-B amorphous catalyst (Ni-Fe-B) was prepared by reducing mixed $FeCl_3$ and $NiCl_2$ with KBH_4 in aqueous solution. At suitable Fe-content (χ_{Fe}), the Ni-Fe-B amorphous catalyst exhibited much higher activity than the corresponding undoped Ni-B in the liquid phase hydrogenation of furfural (FFR) to furfuryl alcohol (FFA). With the increase of χ_{Fe}, the activity first increased and then decreased while the selectivity to FFA changed in a contrast way. The Fe-B amorphous alloy itself was inactive for the FFR hydrogenation. The optimum χ_{Fe} was determined as 0.51, at which the FFA yield reached 100% after reaction for 4 h. Based on various characterizations, the promoting effect of the Fe-dopant was discussed by considering (1) the increase in the surface area, more highly unsaturated Ni active sites, and the more homogeneous distribution of the Ni active sites owing to the presence of Fe_2O_3 as a dopant; (2) the affinity of the Fe^{3+} for the oxygen in the carbonyl group which strengthened the adsorption of the C=O bond by the catalyst and thus facilitated its hydrogenation; (3) the electron donation of the metallic Fe to the metallic Ni, making Fe electron-deficient while Ni electron-enriched which activated the C=O bond towards the hydrogenation.

Keywords: Furfural (FFR); Hydrogenation; Furfuryl alcohol (FFA); Ni-Fe-B amorphous catalyst

1. Introduction

Catalytic hydrogenation of furfural (FFR) is an important industrial reaction since the product furfuryl alcohol (FFA) is widely used in polymers, fine chemicals, and farm chemicals [1,2]. Gas phase hydrogenation is adopted in most companies, while in some countries, e.g. in China, liquid phase hydrogenation is also frequently employed [3–6]. During the hydrogenation of FFR, various products may be produced, as shown in the following reaction route [3]:

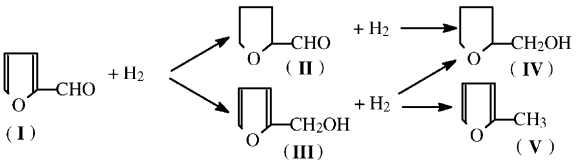

Obviously, the catalyst plays a key role in determining the selectivity to FFA [6]. Up to now, only a few catalysts have been reported for the FFR hydrogenation to FFA [3,7], among them the Cu-Cr based catalysts are most frequently employed. The disadvantage of

* Corresponding author.
E-mail address: hexing-li@shtu.edu.cn (H. Li).

1381-1169/03/$ – see front matter © 2003 Elsevier Science B.V. All rights reserved.
doi:10.1016/S1381-1169(03)00368-6

the Cu-Cr based catalysts is their high toxicity, which causes severe environmental pollution. The Ni-B amorphous alloy has been proved to be an excellent catalyst for many hydrogenating reactions [8–16]. However, it exhibits unsatisfactory activity and especially, the low selectivity to FFA when used in the FFR hydrogenation. It is well known that addition of a transition metal to form a bimetallic catalyst may improve both the activity and selectivity and even the stability during the hydrogenation [17]. This paper reports a novel Fe-promoted Ni-B amorphous catalyst (Ni-Fe-B) which seems powerful in the FFR hydrogenation to FFA.

2. Experimental

2.1. Catalyst preparation

The Ni-Fe-B samples were prepared in the following procedure: at room temperature, 32 ml 2.0 M KBH_4 aqueous solution containing 0.2 M NaOH was added dropwise within 2.0 h into 20 ml $NiCl_2$ aqueous solution containing 1.0 g Ni and a certain amount of $FeCl_3$. The KBH_4 was greatly excessive to ensure the complete reduction of the metallic ions in the solution. During the addition of KBH_4, the solution was stirred vigorously. After complete reaction, the resulting black solid was washed free from Cl^- and K^+ ions as well as some soluble boron species with distilled H_2O (until pH 7 was obtained). Then, it was further washed with absolute alcohol (EtOH) and finally, stored in EtOH until the time of use. The content of the Fe-dopant in the Ni-Fe-B catalyst, expressed in the Fe/(Fe + Ni) molar ratio (χ_{Fe}), was adjusted by changing the amount of $FeCl_3$ in the solution. For comparison, the Ni-B ($\chi_{Fe} = 0$) and the Fe-B ($\chi_{Fe} = 1$) samples were also prepared in the similar way but using single $NiCl_2$ or $FeCl_3$ as the catalyst precursor.

2.2. Catalyst characterization

The amorphous characteristics of the Ni-Fe-B catalysts were investigated by X-ray diffraction (XRD, Bruker AXS D8-Advance with Cu Kα radiation) and selective area electron diffraction (SAED). Differential scanning calorimetry (DSC) was conducted on a SETARAM DSC 111 computer-thermal analysis system under Ar atmosphere with a heating rate of 5 K/min. Alloy compositions were analyzed by means of inductively coupled plasma (ICP, Jarrell-As Scan 2000). BET surface areas (S_{BET}) were measured by nitrogen adsorption at 77 K after degassing at 373 K for 2.0 h. The surface morphology and the particle size were determined by means of both the transmission electron micrography (TEM, JEM-2010) and the scanning electron micrograph (SEM, XL 30 Philips). Ni and Fe K-edge extended X-ray absorption fine structure spectra (EXAFS) were obtained in the National Laboratory of High Energy Physics (BL-10B, KEK, Tsukuba, Japan). Data were treated by using the EXAFS (II) program [18]. The surface electronic states were determined with a X-ray photoelectron spectroscope (XPS, Perkin-Elmer PH I 5000C). Slight Ar^+ sputtering was employed to remove surface impurities. All binding energy (BE) values were calibrated by using the value of contaminant carbon ($C_{1S} = 284.6$ eV) as a reference.

2.3. Activity test

The hydrogenation reaction was carried out in a stainless autoclave containing 10 ml FFR, 30 ml EtOH and 1.0 g catalyst at the reaction conditions of $P_{H_2} =$ 1.0 MPa and $T = 373$ K. The stirring effect was preliminarily investigated and a stirring rate of 1000 rpm was employed, this turned out to be sufficient to eliminate the diffusion limit. According to the drop of H_2 pressure with the time, the hydrogen uptake rates, i.e. the hydrogen consumption per hour and per gram Ni (R_{H_2}, mmol H_2/h g Ni) were calculated according to the ideal gas equation. After reaction for 4 h, the FFR conversion and the selectivity to FFA was measured by gas chromatographic analysis (GC 1102) equipped with a flame ionization detector (FID). The conditions for the analysis were as follows: OV 101 column, injector temperature 373 K, oven temperature 393 K, detector temperature 423 K, and carrier gas N_2, 30 ml/min. In each run of analysis, the total carbon content detected in the reaction mixture was almost the same as that in the initially added FFR, showing that there existed a carbon balance before and after FFR hydrogenation. Thus, one can conclude that no other products were left out during the present GC analysis. The reproducibility of the results was

checked by repeating the runs at least three times on the same batch of catalyst and for another three times for a different batches of catalyst and was found to be within acceptable limits (±5% for the same batch of the catalyst and ±10% for the different batches of the catalyst).

3. Results and discussion

Fig. 1 shows the HRTEM morphology of the as-prepared Ni-Fe-B sample, from which one can see that the Ni-Fe-B sample was present in the form of spherical particles with the average diameter around 30 nm. Those particles were surrounded by a large quantity of white gel-like substances. They could be attributed to both the boron and iron oxides which could be confirmed by XPS spectra, as discussed below. The XRD patterns, as shown in Fig. 2, revealed that all the fresh Ni-Fe-B samples were present in the amorphous structure similar to that of the undoped Ni-B sample, since only one broad peak around $2\theta = 45^\circ$ was observed [19]. After annealing at 873 K in N_2 for 2 h, the original broad peak disappeared and several diffractional peaks corresponding to the crystalline Ni_2B alloy, Fe_2B alloy, Ni-Fe-B alloy, Ni-Fe alloy, and metallic Ni phases appeared, showing that the amorphous structure was thermodynamically metastable [20] and the as-prepared Ni-Fe-B may undergo a crystallization together with a decomposition at high temperature. The weak peaks corresponding

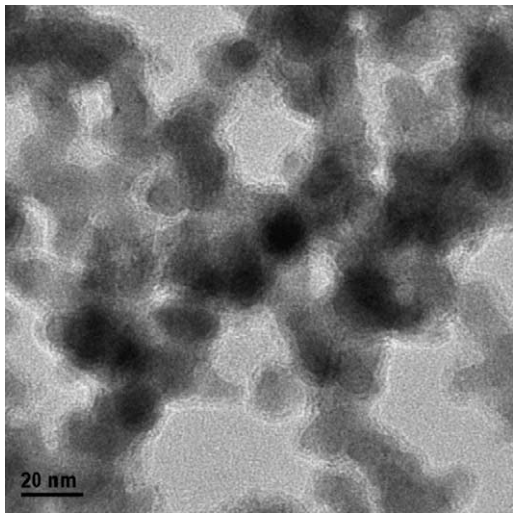

Fig. 1. HRTEM morphology of the fresh Ni-Fe-B sample.

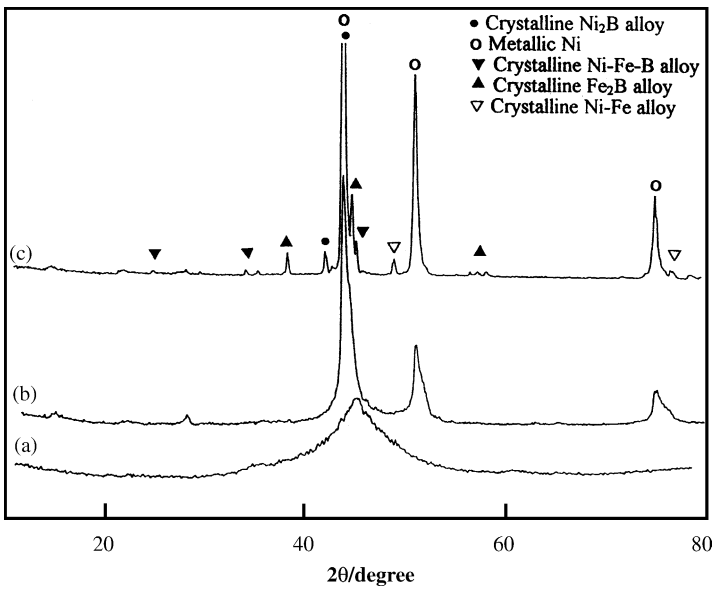

Fig. 2. XRD patterns of the Ni-Fe-B-5 sample ($\chi_{Fe} = 0.51$) treated at different temperatures: (a) as-received; (b) after annealing at 573 K for 2 h in N_2 flow; (c) after annealing at 873 K for 2 h in N_2 flow.

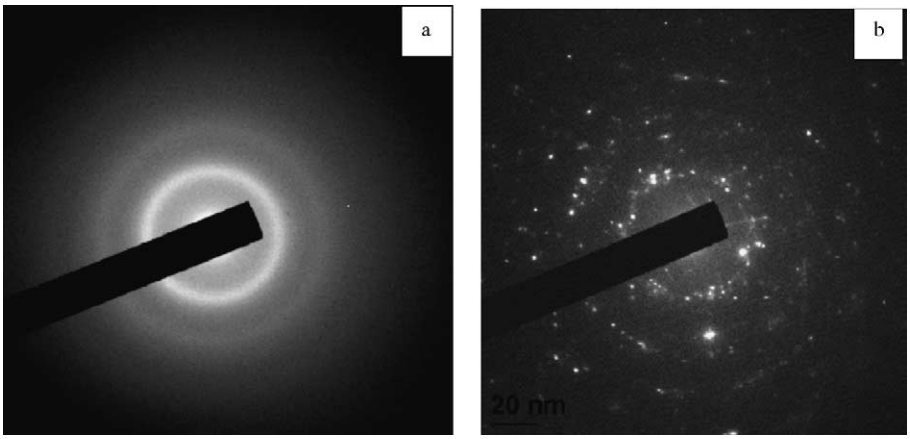

Fig. 3. SAED pictures of (a) the fresh Ni-Fe-B-5 sample and (b) the Ni-Fe-B-5 sample after annealing at 873 K for 2 h in N_2 flow.

to the Fe phases suggested that these Fe species were highly dispersed. The amorphous characteristics of the as-prepared Ni-Fe-B catalysts could be further confirmed by SAED, which displayed various diffractional cycles characteristic of the amorphous structure [21] for the fresh Ni-Fe-B sample and only some bright points after being treated at 873 K for 2 h, as shown in Fig. 3. The DSC analysis, as shown in Fig. 4, demonstrated that the crystallization temperature (T_C) strongly depended on χ_{Fe}. The T_C increased rapidly with the increase of χ_{Fe}, as summarized in Table 1, showing the stabilizing effect of the Fe-dopant on the amorphous structure, possibly due to the effective inhibition of the migration and gathering of catalyst particles, which were essential for the crystallization of amorphous alloys [22,23].

Fig. 5 shows the XPS spectra of the Ni-Fe-B amorphous alloy in Ni_{2P}, Fe_{2P} and B_{1S} levels, respectively. One can see that almost all the Ni species were present in the metallic state corresponding to the binding energy of 852.7 eV [24]. However, the Fe species were present in both the metallic state and the oxidized state (Fe_2O_3) corresponding to BE of 707.1 and 711.2 eV, respectively [25]. Such Fe_2O_3 species could

Table 1
Structural properties of the as-prepared Ni-Fe-B amorphous catalysts

Catalysts	Composition (at.%)	χ_{Fe}[a] (molar ratio)	S_{BET} (m^2/g)	T_C[b] (K)	Ni K-edge EXAFS in first shell		
					N[c]	R[d]	σ[e]
Ni-B	$Ni_{72.2}B_{27.8}$	0	27.2	341	8.6	2.45	0.0064
Ni-Fe-B-1	$Ni_{64.1}Fe_{7.8}B_{28.1}$	0.11	27.5	344	8.6	2.44	0.0067
Ni-Fe-B-2	$Ni_{60.4}Fe_{11.5}B_{28.1}$	0.16	29.4	378	8.2	2.46	0.0072
Ni-Fe-B-3	$Ni_{56.5}Fe_{15.5}B_{28.0}$	0.21	30.2	422	–	–	–
Ni-Fe-B-4	$Ni_{53.7}Fe_{18.9}B_{28.4}$	0.26	32.1	465	–	–	–
Ni-Fe-B-5	$Ni_{34.1}Fe_{36.0}B_{29.9}$	0.51	32.9	556	7.2	2.45	0.0084
Ni-Fe-B-6	$Ni_{23.1}Fe_{48.1}B_{28.8}$	0.68	34.1	589	–	–	–
Ni-Fe-B-7	$Ni_{17.3}Fe_{54.4}B_{28.3}$	0.76	35.6	611	6.4	2.44	0.0073
Ni-Fe-B-8	$Ni_{14.2}Fe_{58.0}B_{27.8}$	0.80	37.6	626	6.3	2.43	0.0066
Fe-B	$Fe_{73.0}B_{27.0}$	1.0	41.3	705	–	–	–

[a] Fe/(Ni + Fe) molar ratio.
[b] Crystallization temperature obtained by DSC analysis.
[c] N: coordination number.
[d] R: interatomic distance (Å).
[e] σ: D–W factor (nm).

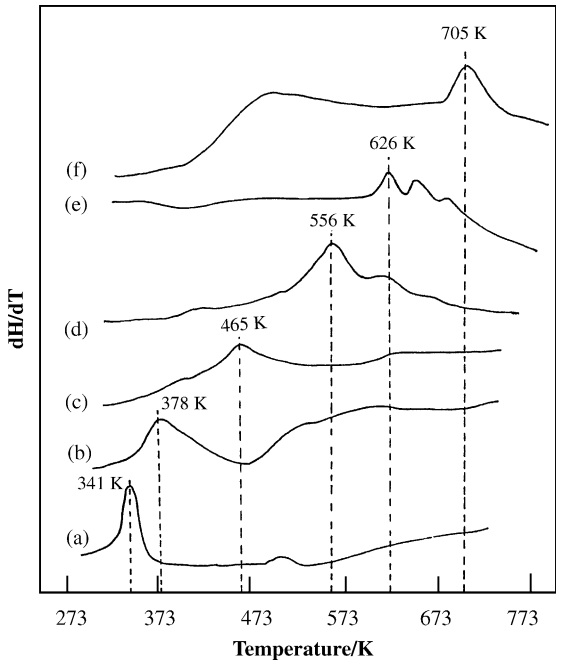

Fig. 4. DSC curves of: (a) Ni-B; (b) Ni-Fe-B-2; (c) Ni-Fe-B-4; (d) Ni-Fe-B-5; (e) Ni-Fe-B-8; and (f) Fe-B samples obtained under the same preparation conditions.

be effectively removed when the sample was treated with dilute ammonia solution. However, the Ar^+ sputtering could not remove these Fe_2O_3 species, showing that they were not produced from the surface oxidation. The Fe_2O_3 species may be formed via the hydrolysis of Fe^{3+} ions taking into account that the KBH_4 solution containing 0.2 M NaOH was strongly alkaline. Similarly, the B species were also present in two states, the alloying B and the oxidized B (B_2O_3) corresponding to BE values of 188.0 and 192.5 eV, respectively [24]. The BE of the alloying B positively shifted by 0.9 eV in comparison with the standard BE of the pure B (187.1 eV) [24]. Similarly, by comparing with the standard BE of pure Fe metal (706.6 eV) [25], it was also found that the metallic Fe in the Ni-Fe-B sample shifted positively by 0.5 eV. These results demonstrated that partial electrons transferred from both Fe and B to Ni in the Ni-Fe-B amorphous alloy, i.e. the alloying B and metallic Fe were electron-deficient while the metallic Ni was electron-enriched. The electronic interaction between the alloying B and the metallic Ni in the Ni-B amorphous alloy has been well stud-

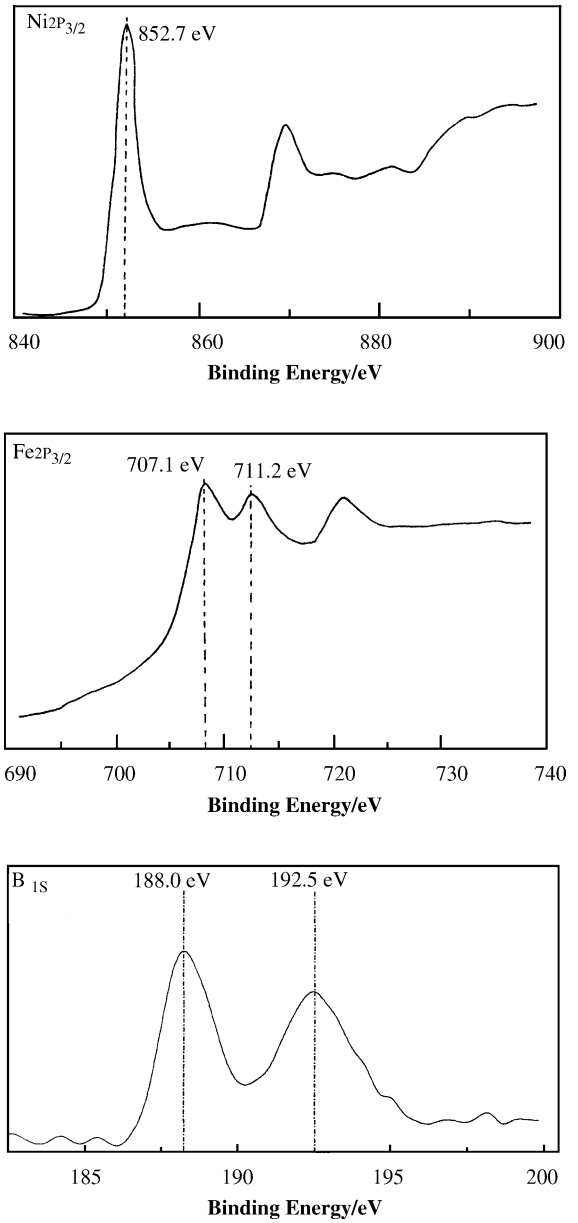

Fig. 5. XPS spectra of the Ni-Fe-B-5 amorphous alloy catalyst in $Ni2P_{3/2}$, $Fe2P_{3/2}$, and B_{1S} levels, respectively.

ied [15,26–31], while, by using soft X-ray appearance potential spectroscopy, Chouresia and Chopra also confirmed the electron transfer from Fe to Ni in the Ni-Fe alloy [32]. In our previous papers [24], we reported that, because of the larger size of Ni

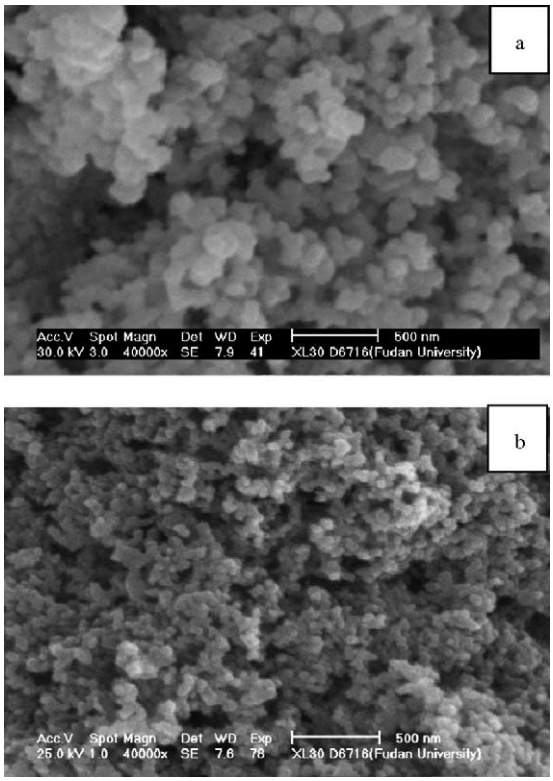

Fig. 6. SEM morphologies of (a) the fresh Ni-B and (b) the fresh Ni-Fe-B-5 samples obtained under the same preparation conditions.

atom than that of B, the BE of the metallic Ni in the Ni-B amorphous alloy remained almost unchanged comparing to the standard BE value of the pure Ni metal (853.1 eV) even though B donated partial electrons. However, significant BE shift of the metallic Ni (ca. 0.4 eV) was observed in the Ni-Fe-B sample, showing that the Ni atom got more electrons since the Fe-dopant donated additional electrons besides the alloying B.

Table 1 shows the effect of the Fe-dopant on the physical properties of the as-prepared Ni-Fe-B amorphous catalysts. The change of χ_{Fe} had very little influence on the boron content. However, the surface area (BET) of the Ni-Fe-B sample increased considerably with the increase of χ_{Fe}, which was mainly attributed to the decrease in the particle size owing to the dispersing effect of the Fe_2O_3 support. This was strongly supported by the SEM morphologies, as shown in Fig. 6. Based on the calculations from the Ni K-edge EXAFS data, it was found that the change of χ_{Fe} had no significant effect on the inter-atomic distance (R). However, the coordination number (N) decreased with the increase of χ_{Fe}, showing that the Ni active sites became more highly unsaturated owing to decrease in the particle size. The D–W factor (σ), which represents the disordering term in the nearest neighbors, first increased and then decreased with the increase of χ_{Fe}. The maximum σ was obtained at $\chi_{Fe} = 0.51$, showing that the presence of suitable amount of the Fe-dopant may favor the homogeneous distribution of the Ni active sites [26].

At extremely low content ($\chi_{Fe} < 0.11$), no significant effect of the Fe-dopant on both the structural and electronic characteristics of the as-prepared Ni-Fe-B amorphous catalyst was observed. A possible explanation is that, at extremely low content, these Fe atoms were mainly present as isolated atoms in the Ni lattice rather than as the alloying Fe with Ni [33].

Figs. 7 and 8 show the dependence of the FFR conversion, the selectivity to FFA, and the RH_2 on χ_{Fe}, from which the following results could be obtained:

1. Effect the Fe-dopant on the activity. With the increase of χ_{Fe}, the activity of Ni-Fe-B amorphous catalysts first increased and then decreased. The maximum activity was obtained at $\chi_{Fe} = 0.51$. As the Fe-B amorphous alloy itself was inactive for the FFR hydrogenation, one might conclude that only the metallic Ni served as the active site in the Ni-Fe-B amorphous alloy and the Fe-dopant served as a promoter. As discussed above, the addition of very small amount of the Fe-dopant ($\chi_{Fe} < 0.11$) had no significant effect on both the structural and the electronic characteristics of the Ni-Fe-B catalyst. Thus, the promoting effect of the Fe-dopant at such a low content could be attributed to the presence of isolated Fe atoms in the Ni lattice. Yadav and Kharkara [33] found that, the Fe atoms in the Ni lattice were more active than the Ni atoms. At χ_{Fe} from 0.11 to 0.51, the promoting effect of the Fe-dopant may be accounted by considering the presence of both the metallic Fe and the Fe_2O_3. Concerning the role of the metallic Fe, the aforementioned XPS spectra revealed that the metallic Fe donated partial electrons to Ni similar to that of the alloying B. On one hand, the electron-deficient Fe could attract the oxygen in the carbonyl group

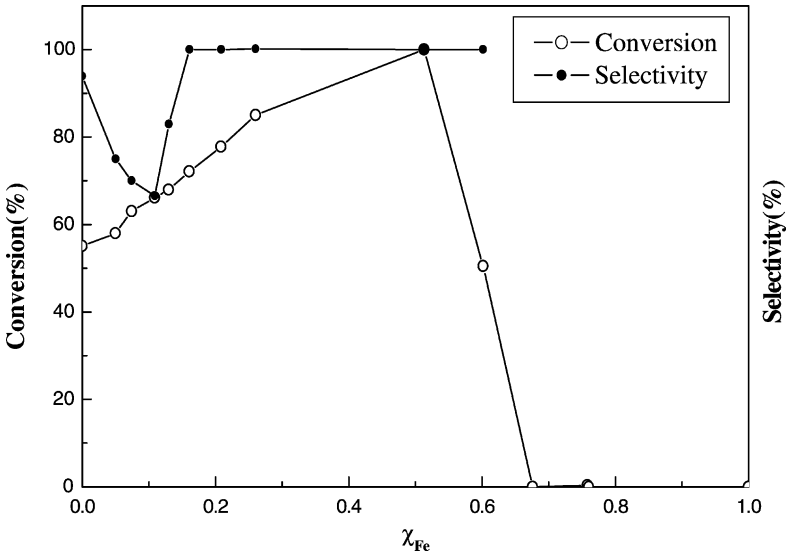

Fig. 7. Dependence of the FFR conversion (○) and the selectivity to FFA (●) on the Fe-content (χ_{Fe}) during the liquid phase FFR hydrogenation over the Ni-Fe-B amorphous alloy catalysts. Reaction conditions: 10 ml FFR, 30 ml EtOH, 1.0 g catalyst, $T = 373$ K, $P_{H_2} = 1.0$ MPa, stirring rate = 1000 rpm, reaction time = 4 h.

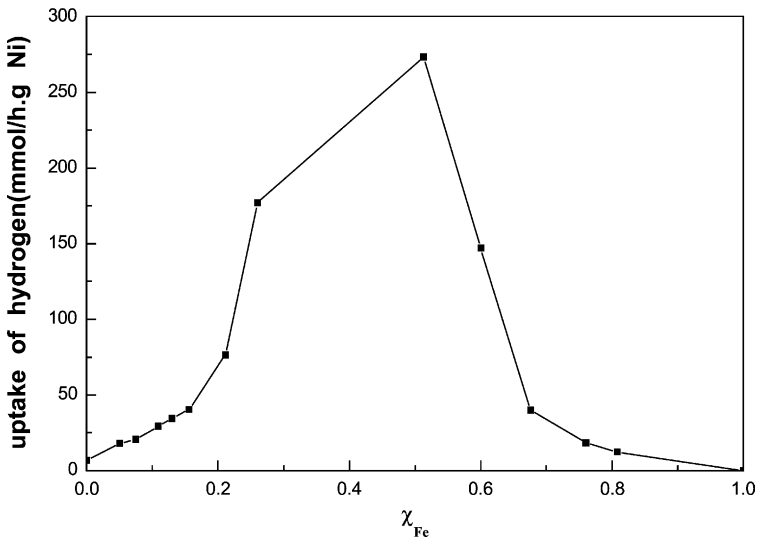

Fig. 8. Effect of the Fe-content (χ_{Fe}) on the specific activity of the Ni-Fe-B amorphous alloy catalysts in the liquid phase hydrogenation of FFR. Reaction conditions are given in Fig. 7.

via a side-bond interaction [34–36], as shown in the following model, which might weaken and activate the C=O bond π-complexed to the Ni atom and in turn promote the hydrogenation of the C=O bond.

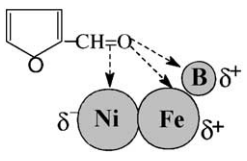

On the other hand, according to the studies on the CO adsorption on transition metals [37,38], the primary interactions are the forward donation from the highest occupied molecular orbital (HOMO) of C=O, i.e. from 5σ to the surface d_{z^2} and s states, and the back donation from metal $d_{x^2-y^2}$ to the lowest unoccupied molecular orbital (LUMO) of C=O, i.e. $2\pi^*$. As $2\pi^*$ is an antibonding orbital, increased back donation from the metal could weaken the C=O bond and thus, favors the dissociation of the C=O bond. Since the metallic Ni was more electron-enriched in the presence of the Fe-dopant, the Ni active sites became more electrons would back donate from Ni to $2\pi^*$ of the C=O bond which also facilitated the hydrogenation of C=O bond. Concerning the role of Fe_2O_3, it is well known that the affinity of the Fe^{3+} for the oxygen in the carbonyl group might also activate the C=O bond [39]. Meanwhile, the Fe_2O_3 could serve as a support that enhanced the surface area, created the more highly unsaturated Ni active sites and also promoted the more homogeneous distribution of these Ni active sites, as shown in Table 1. All these factors were favorable for the hydrogenation activity [13]. At very large concentration of the Fe-dopant, the activity decreased again since too many surface Ni active sites would be covered by the inactive Fe species.

2. Effect of the Fe-dopant on the selectivity. Under the present conditions, the main byproduct was determined as tetrahydrofurfural (HFFR), resulting from the competitive hydrogenation of the furan ring, as shown in the above reaction route. Addition of small amount of the Fe-dopants ($\chi_{Fe} < 0.11$) may facilitate the formation of HFFR, resulting in an abrupt drop in the selectivity to FFA. This could be attributed to presence of the isolated Fe atoms existed in the Ni lattice. They were so active that both the C=O group and the furan ring could be hydrogenated [24]. When χ_{Fe} further increased, the selectivity to FFA regained and increased rapidly up to 100% at $\chi_{Fe} = 0.16$. Besides the coverage of the isolated Fe atoms originally existed in the Ni-lattice, the promoting effect of the Fe-dopant on the selectivity could be mainly attributed to both the metallic Fe and Fe_2O_3. As discussed above, both the electron-deficient Fe atoms and the Fe^{3+} species could activate the C=O bond via a side-bond adsorption of the oxygen in carbonyl group. Meanwhile, the more electron-enriched Ni atoms could also activate the C=O bond due to the more back donation of the electrons from the Ni atom to the $2\pi^*$ antibonding orbitals of the C=O group. Thus, with the increase of χ_{Fe}, the hydrogenation of the C=O group became easier than that of the furan ring, resulting in the higher selectivity to FFA.
3. Effect of the alloying boron on the catalytic behaviors. In our previous paper [40], the catalytic behaviors of both the Ni-B amorphous alloy catalyst prepared from the reduction of Ni^{2+} with KBH_4 and the Ni powder catalyst obtained from the reduction of Ni^{2+} with NH_2NH_2 were investigated in details during the liquid phase FFR hydrogenation. The Ni-B amorphous alloy catalyst exhibited much higher activity and better selectivity to FFA than the Ni powder catalyst, showing the promoting effect of the alloying B on both the activity and selectivity to FFA which could be understood by considering both the structural effect and electronic effect. Briefly, concerning the structural effect, the presence of the alloying B resulted in the amorphous alloy in the Ni-B catalyst while only the crystalline structure was obtained without the alloying B, as determined in the Ni powder catalyst. It has been widely accepted that such amorphous alloy structure was favorable for both the activity and selectivity and even the sulfur resistance in many hydrogenation reactions owing to the stronger synergistic effect between active sites, the more highly unsaturated active sites, and the more homogeneous distribution of these active sites [13,26]. Regarding the electronic effect, the XPS spectra revealed that there was strong electronic interaction between metallic Ni and the alloying B, in which the alloying B donated partial electrons to metallic Ni, making Ni electron-enriched, just similar to the metallic Fe in the present Ni-Fe-B amorphous alloy catalyst. Thus, the promoting effect of the alloying B could be explained in the similar way to that of the metallic Fe as discussed above.

4. Conclusions

At suitable content of the Fe-dopant (χ_{Fe}), the Fe-doped Ni-B amorphous alloy catalyst exhibited

higher activity and better selectivity to FFA during the liquid phase FFR hydrogenation. The optimum χ_{Fe} was determined as 0.51. The promoting effect of the Fe-dopant on the selectivity to FFA could be mainly attributed to the activation of the C=O bond by both the electron-deficient Fe and the Fe^{3+}. Meanwhile, the electron-enrichment of the Ni active sites could also weaken the C=O bond by a back donation of electrons to the antibonding orbital ($2\pi^*$) of the carbonyl group. Such electronic effect, together with the dispersing effect of the Fe_2O_3, could also explain the promotion of the Fe-dopant on the hydrogenation activity. Very low content of the Fe-dopant ($\chi_{Fe} < 0.11$) was harmful for the selectivity to FFA because the isolated Fe atoms existed in the Ni lattice so active that both the carbonyl group and the furan ring could be hydrogenated. Meanwhile, very high content of the Fe-dopant ($\chi_{Fe} > 0.51$) was harmful for the activity because too many Ni active sites are covered by the inactive Fe and Fe_2O_3 species. The maximum FFA yield (100%) could be obtained over the Ni-Fe-B amorphous alloy catalyst with $\chi_{Fe} = 0.51$ after reaction for 4 h under the present conditions.

Acknowledgements

This work was supported by the National Natural Science Foundation of China (29973025, G2000048009), the Natural Science Foundation of Shanghai Science and Technology Committee (00XD14019), and the Educational Department of P.R. China.

References

[1] K. Bauer, D. Garbe, Common Fragrance and Flavor Materials, VCH, Kyoto, Japan, 1985.
[2] M.S. Li, W.Z. Ma, Hebai Ind. (1999) 6.
[3] R.S. Rao, R.T.K. Baker, M. Vannice, Catal. Lett. 60 (1999) 51.
[4] B. Liu, L. Lu, B. Wang, T. Cai, I. Katsuyoshi, Appl. Catal. A: Gen. 171 (1998) 117.
[5] De Thomas, US Patent 4153578 (1979).
[6] H.S. Luo, H.X. Li, L. Zhuang, Chem. Lett. (2001) 138.
[7] Z. Huang, L. Qiu, Shiyou Huagong 21 (1992) 35.
[8] H. Li, H.X. Li, W.J. Wang, J.F. Deng, Chem. Lett. (1999) 629.
[9] H.X. Li, W.J. Wang, J.F. Deng, J. Catal. 191 (2000) 257.
[10] H.X. Li, Y.P. Xu, H. Li, J.F. Deng, Appl. Catal. A: Gen. 216 (2001) 51.
[11] H.X. Li, X.F. Chen, M.H. Wang, Y.P. Xu, Appl. Catal. A: Gen. 225 (2002) 117.
[12] X.B. Yu, M.H. Wang, H.X. Li, Appl. Catal. A: Gen. 202 (2000) 17.
[13] A. Baiker, Faraday Discuss. Chem. Soc. 87 (1989) 239.
[14] A. Molnar, G.V. Smith, M. Bartok, Adv. Catal. 36 (1989) 329.
[15] J.F. Deng, H.X. Li, W.J. Wang, Catal. Today 51 (1999) 113.
[16] S. Linderoth, S. Morup, J. Appl. Phys. 69 (1991) 5256.
[17] A.J. den Hartog, V. Ponec, Stud. Surf. Sci. Catal. 54 (1990) 173.
[18] J. Chen, G. Lu, L. Ma, Fudan Univ. Acta 28 (1989) 78.
[19] H. Yamashita, M. Yoshikawa, T. Funabiki, S. Yoshida, J. Chem. Soc. Faraday Trans. I 81 (1985) 2485.
[20] H.X. Li, W. Wang, H. Li, J.F. Deng, J. Catal. 194 (2000) 211.
[21] S. Klein, J.A. Martens, R. Parton, K. Vercruysse, P.A. Jacobs, W.F. Maier, Catal. Lett. 38 (1996) 209.
[22] X.F. Chen, H.X. Li, M.H. Wang, Y.P. Xu, Appl. Catal. A: Gen. 233 (2002) 13.
[23] H. Yamashita, M. Yoshikawa, T. Funabiki, S. Yoshida, J. Catal. 99 (1986) 375.
[24] H. Li, H.X. Li, W. Dai, Z. Fang, J.F. Deng, Appl. Surf. Sci. 152 (1999) 25.
[25] C.D. Wager, W.H. Riggs, L.E. Davis, J.F. Moulder, G.E. Meilenberg, Handbook of X-Ray Photoelectron Spectroscopy, Perkin-Elmer Coorperation, Physical Electronic Division, Eden Prairie, MN, 1979.
[26] B. Shen, S. Wei, K. Fan, J.F. Deng, Appl. Phys. A 65 (1997) 295.
[27] Y. Okamoto, Y. Nitta, T. Imanaka, S. Teranishi, J. Chem. Soc. Faraday Trans. 1 76 (1980) 998.
[28] S. Yoshida, H. Yamashita, T. Funabiki, T. Yonezawa, J. Chem. Soc. Faraday Trans. 1 80 (1984) 1435.
[29] W. Dai, H.X. Li, Y. Cao, M.H. Qiao, K.N. Fan, J.F. Deng, Langmuir 18 (2002) 9605.
[30] Y. Okamoto, Y. Nitta, T. Imanaka, S. Teranishi, J. Chem. Soc. Faraday Trans. 1 75 (1979) 2027.
[31] T. Imanaka, Y. Nitta, S. Teranishi, Bull. Chem. Soc. Jpn. 46 (1973) 1134.
[32] A.R. Chouresia, D.R. Chopra, Surf. Sci. 206 (1988) 484.
[33] G.D. Yadav, M.R. Kharkara, Appl. Catal. A: Gen. 126 (1995) 115.
[34] Y.Z. Chen, S.W. Wei, K.J. Wu, Appl. Catal. A: Gen. 99 (1993) 85.
[35] F. Delbecq, P. Sautet, J. Catal. 152 (1995) 217.
[36] G. Szollosi, B. Torok, G. Szakonyl, I. Kun, M. Bartok, Appl. Catal. A: Gen. 172 (1998) 225.
[37] R. Hoffman, S.S. Sung, J. Am. Chem. Soc. 101 (1985) 578.
[38] E. Boellaard, R.J. Vreeburg, O.L.J. Gijzeman, J.W. Geus, J. Mol. Catal. 92 (1994) 299.
[39] A. Fukuka, T. Kimura, N. Karugi, H. Kuroda, Y. Minai, Y. Sakai, T. Tominaga, M. Ichikana, J. Catal. 126 (1990) 434.
[40] H. Luo, L. Zhuang, H.X. Li, J. Mol. Catal. (Chin.) 16 (2002) 49.